Study on leaching kinetics of laterite ore using hydrochloric acid

Jinhui Li, Zhifeng Xu, Ruixiang Wang, Yang Gao, Yang Yang

School of Metallurgical and Chemical Engineering, Jiangxi University of Science and Technology, Ganzhou, 341000, P.R. China

Corresponding authors: jinhuili@jxust.edu.cn (J.H. Li), fafa_1i@163.com (Z.F. Xu)

Abstract: The process of atmosphere-pressure acid leaching of laterites has attracted considerable attention in the nickel industry in recent years. However, the leaching kinetics of laterite using hydrochloride acid has not yet been fully researched. In this paper, the mineral analysis of the ore was carried out, and the leaching mechanism of different minerals at different time was studied comprehensively. The kinetics analysis of the leaching process of nickel, cobalt and manganese showed that the kinetics model of diffusion controlling was suitable and could be described by the linear equation, $1-3(1-a)^{2/3}+2(1-a)=k_2t$. Based on the linear equation and the Arrhenius equation, the values of activation energy of metal leaching can be deduced (11.56 kJ/mol for nickel, 11.26 kJ/mol for cobalt and 10.77 kJ/mol for manganese). Study of leaching mechanism shows that the order of these minerals dissolution is: goethite, lizardite, magnetite and hematite. Due to the original or product of silica, magnetite, hematite and talc, they can form the solid film which hinders the leaching of valuable metals. Thus, the diffusion controlling step is inner diffusion, namely solid film diffusion controlling.

Keywords: nickel laterite, hydrochloride acid, kinetics analysis, hydrometallurgy, leaching mechanism

1. Introduction

Nickel (Ni) is an important metal in modern infrastructure and technology, which has been widely used in stainless steel (~58%), nickel-based alloys (~14%), casting and alloy steels (~9%), electroplating (~9%) and rechargeable batteries (~5%) (Zhao et al., 2017; Li et al., 2015). Nickel can be commonly found in two principal ore types-sulfide and laterite ores. Although about 70% of the world land-based nickel resource is stored in laterite, only about 40% of world nickel production is from laterite in the past years. Compared with processing of sulfide-laterite ores, nickel laterite processing requires extensive and complex treatment to extract nickel, leading to higher costs (Kevin et al., 2011). Unlike sulfide ores, laterite cannot be significantly upgraded and concentrated for processing, since the distribution of nickel throughout the molecular lattice of the particles makes the production of a concentrate by flotation or gravity separation impractical. It essentially means that nearly every tone of laterite ore mined must be went through the entire process, resulting in higher operating costs (Norgate and Jahanshahi, 2011). To meet future demand for Ni, however, an increasing amount of Ni has been mining from laterite ores (Gavin M. Mudd, 2010; Ma et al., 2015; Nevill Matson Rice, 2016).

The hydrometallurgical treatment of laterite minerals is increasingly important, as it is expected that the nickel and cobalt production will mostly obtained through hydrometallurgical processe in the future (McDonald and Whittington, 2008a,b). Conventionally, sulfuric acid pressure leaching (PAL) process has developed into the preferred route to extract nickel and cobalt from laterites (mostly limonite) due to the easy precipitation of iron during the leaching process (BÜYÜKAKINCI and Topkaya, 2009; MacCarthy et al., 2016). However, the major drawbacks of the PAL process are high capital cost, high operating cost, plenty of residual acid and expensive materials construction at commercial level (McDonald and Whittington, 2008a,b).

In the leaching process, hydrochloric acid as the leachant is preferred because of comparatively easier recovery of the useful free acid from its waste solution and solvent extraction (SX) in chloride medium than does sulphuric acid (Lakshmanan et al., 2016). Although chloride-based commercial leaching operations are not common, more and more relative researches have been introduced (Zhang et al., 2016; Liu et al., 2010; Fan et al., 2011).

Kinetics study is an essential part in designing a leaching process, and the major models that have been developed for kinetics of non-catalytic liquid-solid reactions are the shrinking (including shrinking particle and shrinking core), homogeneous, grain, uniform pore and random pore models (Zhang et al., 2017). Some groups have systematically studied the leaching kinetics mainly focusing on sulfuric acid and some special minerals of laterite (Olanipekun, 2000; Liu et al., 2012; Luo et al., 2010).

In this investigation, the laterite ore from China is mixture from three layers of a mine, but not single type laterite. It's noteworthy thatthis type of laterite ores has been used in many factories. In addition, the leaching process using hydrochloride acid was applied by more and more factories. Therefore, the results in this paper will substantially support the basis theory in industry. In this paper, this mixed laterite ore was used in experiments to study kinetics, and the leaching conditions have been discussed in previous work. The effects of several important parameters including temperature, stirring speed and particle size were discussed. Mineralogical analysis of the raw laterite and the leaching residues were carried out to study the leaching mechanism. The dissolution order of minerals was also investigated to understand the function of the stability of different minerals in the kinetics analysis.

2. Materials and methods

2.1. Material analysis

The ores tested in this study are khaki color and block, originated from Yunnan province in China, where the laterite mainly consists of three layers in order of increasing depth: a hematite cap, a limonitic laterite deposit and finally garnieritic ore. After drying in vacuum overnight at 105 °C, the ores were ground to 100% passing different meshes. Chemical analysis of the dried lateritic ores was carried out with chemical analysis, Inductively Coupled Plasma (ICP) and X-Ray Fluorescence (XRF). Mineralogical study was carried out in main minerals using a Rint-2000 X-ray diffractometer (XRD) with Cu Kα radiation from 5° to 85° (2θ) and a TSU-70C optical microscope.

2.2. Apparatus and procedures

A 50 g of ore was added into the leaching solution in a 500-mL three-necked, round-bottomed flask, which were placed on a temperature controlled and magnetically stirred water bath equipped with a digitally controlled thermometer (within±0.5 °C). A condenser was used to avoid evaporation losses during leaching process as shown in Fig. 1.
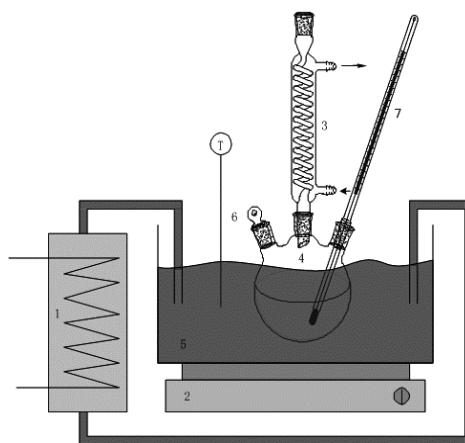

Fig. 1. Leaching equipment sketch (1. temperature-controlled bath with external flow, 2. magnetic stirrer, 3.tap water-cooled condenser, 4. round-bottom flask with 3 holes, 5. water bath, 6. outlets for batch addition and solution sampling, 7. thermometer)

Prepared leach solution of the desired concentration of hydrochloric acid was placed into the glass balloon. Once the desired temperature was reached, the ore sample was added from the feed opening and stirred at a constant speed by a Teflon coated magnet for the required duration. At the end of leaching, the leached ore was filtered and washed with distilled water using a Büchner funnel. Pregnant and wash water solutions were collected and kept constant recovery. The effect of leaching duration on different metals extraction was investigated comprehensively, and the result can be calculated using Eq. 1, where the leaching time was counted from the time of ore addition:

$$X_{M,i} = \frac{\left(V - \sum_{i=1}^{i-1} v_i\right)C_{M,i} + \sum_{i=1}^{i-1} v_i C_{M,i}}{m(c_M/100)}$$

(1)

where X is the metal dissolution, M represents metal, V is the initial volume (ml) of the solution, v_i is the volume (ml) of the sample i withdrawn each time, $C_{m,i}$ is the concentration of M in sample i (mg/L), m is the initial mass of laterite (g) (on dried basis) added into the reactor and Cm is the concentration of M in laterite (wt% dried solids).

The volumetric analysis ($K_2Cr_2O_7$ titration) was employed for Fe, Ni, Co and Mn were analyzed with the help of ICP. Leach residues were dried at 105 °C, weighed and analyzed by XRD. Reagent grade chemicals and de-ionized water were used in these experiments.

3. Results and discussion

3.1. Mineralogical analysis

The components of raw ore were identified by XRD from 5° to 85° (Fig. 2). As characterized by XRD, the main minerals are lizardite ($Mg_3Si_2(OH)_4O_5$), goethite (FeO(OH)), hematite (Fe_2O_3), magnetite (Fe_3O_4) and quartz (SiO_2). Analysis of optical microscope shows that about 0.002 mm particle size of goethite is cocooned and distributes in magnetite minerals (Fig. 3), and maghemite (white) and limonite (gray) located in other minerals are detected (Fig. 4). The size of maghemite is below 0.01 mm, and the size of limonite is between 0.05 and 0.3 mm.
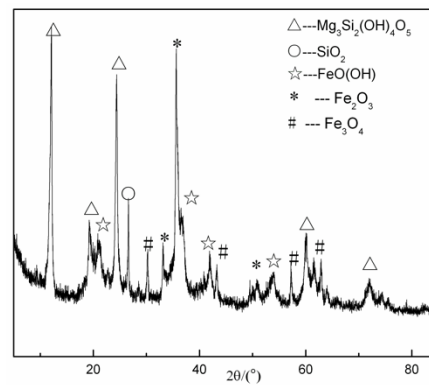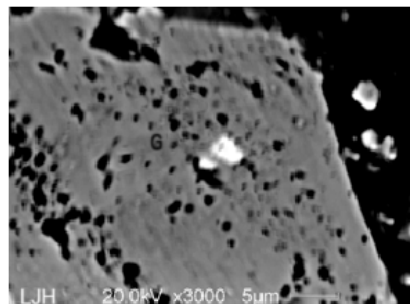

Fig. 2. Powder XRD pattern of raw laterite

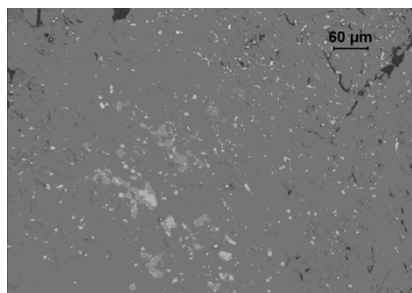Fig. 3. Fine goethite (white) in magnetite mineral

Fig. 4. Fine maghemite (white) and limonite (gray) located in gangue

The result of chemical analysis is shown in Table 1. It can be found that the main valuable metals of Ni and Co are distributed in different minerals, such as goethite, limonite, sulfite and lizardite, shown in Tables 2 and 3. Ni is mainly existed in iron minerals (about 86%) and Co is about 65% in iron minerals, which show that the leaching of Ni and Co would lead iron leaching correspondingly. Considering the result of Figs. 3 and 4, the ore must be ground to small particle size, so as to increase the reaction probabilities between iron minerals and the leaching solution.

Table 1. Chemical composition of raw ore

Constituent	NiO	CoO	MnO	Fe_2O_3	CuO	MgO	Al_2O_3	SiO_2
Content (wt.%)	0.60	0.042	0.171	15.01	0.007	26.4	0.34	57.43

Table 2. The distribution of nickel in main minerals of the ore

Ni phase	Goethite	Limonite	Sulfide	Lizardite	Total
Content (wt.%)	0.46	0.25	0.02	0.14	0.87
Distribution rate(%)	69.18	16.97	1.64	12.21	100.00

Table 3. The distribution of cobalt in main minerals of the ore

Cobalt phase	Goethite	Limonite	Sulfide	Lizardite	Total
Content (wt.%)	0.0306	0.017	0.0081	0.0053	0.061
Distribution rate(%)	49.55	15.23	9.20	26.02	100.00

3.2. Kinetics Analysis

In previous work, the optimum leaching conditions have been studied comprehensively. The dissolution of nickel, cobalt, manganese, magnesium and iron were 92.3 wt.% and 61.5 wt.%, 93.5 wt.%, 95.5 wt.% and about 56.3 wt.% at the leaching conditions of acid concentration (8 mol/L), particle size of samples (100% passing 0.15 mm), agitating rate (300 rpm), the temperature (353 K), S/L ratio (1:4) and leaching time (2 hours). Taking into account that the ore consisted of essentially dense grains which could be viewed as nonporous particles, and that the ore grains gradually shrunk and the product layer formed around the unreacted grains during leaching, shrinking core model was selected in this study. Because it was more suitable to the leaching of nonporous solids, and the other models such as homogeneous, grain and pore models were usually applied to the porous solid–liquid system.

To determine the activation energy of main metals, a series of leaching experiments were carried out. The results presented in Figs. 5, 6 and 7 show that the leaching rates were influenced by temperature.

For main metals dissolution kinetics, one previously established shrinking core models were used, expressed by the following equations:

$$1-(1-a)^{1/3}=k_1 t \tag{2}$$

$$1-3(1-a)^{2/3}+2(1-a)=k_2t \tag{3}$$

where a is the fraction of metal dissolved at time t, k_1 and k_2 are the overall rate constants. Eq. (2) assumes that the rate-controlling step of the leaching is the chemical reaction taking place on the surface of the mineral, and Eq. (3) assumes that the controlling step is the diffusion through the product layer.
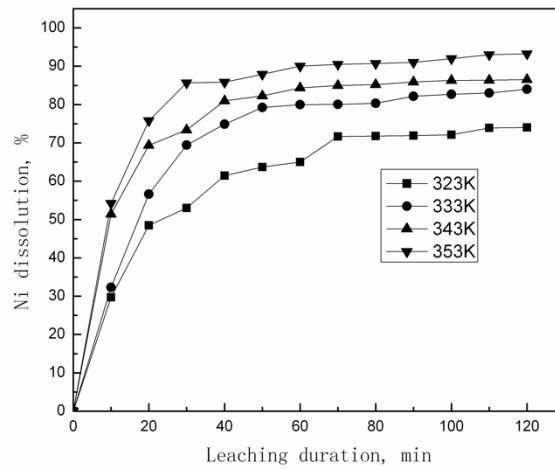

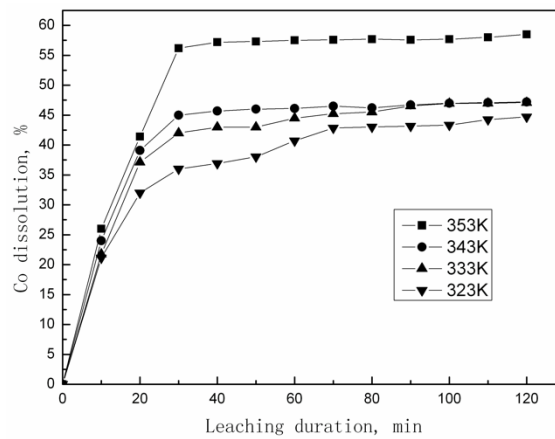Fig. 5. Leaching duration on Ni dissolution at different temperatures

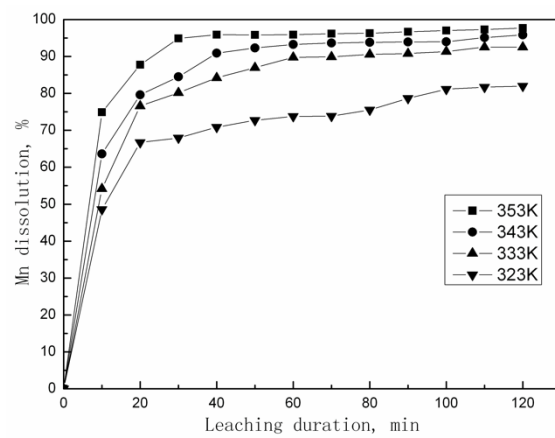Fig. 6. Leaching duration on Co dissolution at different temperatures

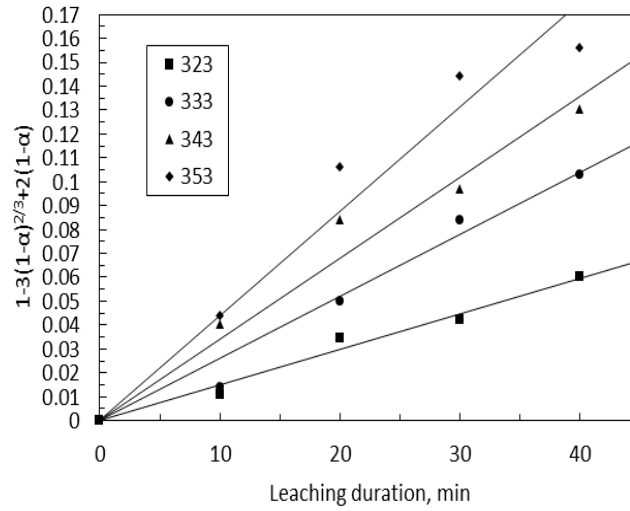Fig. 7. Leaching duration on Mn dissolution at different temperatures

Fig. 8. Plots of $1-3(1-a)^{2/3}+2(1-a)$ vs. leaching duration of Ni for different temperatures
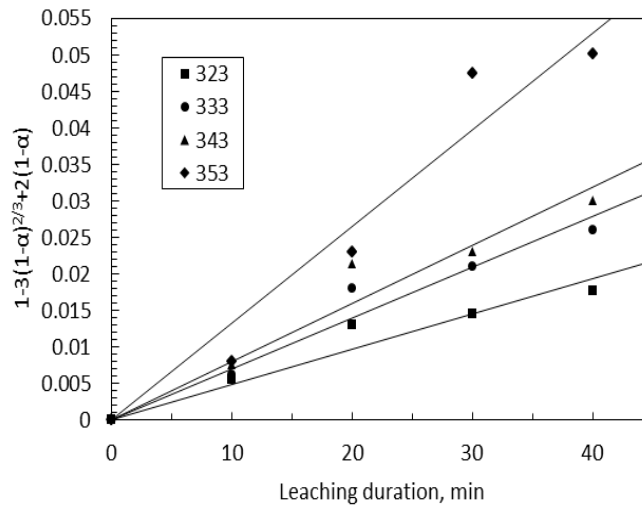

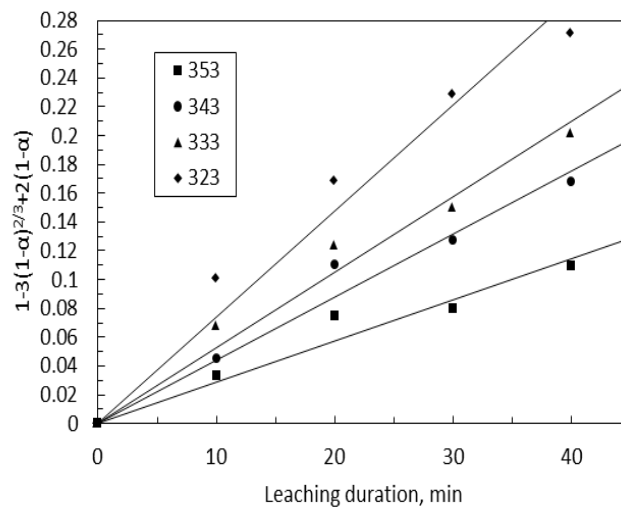Fig. 9. Plots of $1-3(1-a)^{2/3}+2(1-a)$ vs. leaching duration of Co for different temperatures

Fig. 10. Plots of $1-3(1-a)^{2/3}+2(1-a)$ vs. leaching duration of Mn for different temperatures

Although the optimum leaching duration was 2 hours, the leaching rate increased slowly after 40 minutes which were shown in Figs. 5, 6 and 7. So the emphasis of kinetics research was focused on the former period. And the leaching rate increased obviously with the raise of temperature for nickel, cobalt and manganese in the same reaction duration. Examination of the plots of the above kinetics equations as functions of time showed that only Eq. (3) gave perfect straight lines as shown in Figs. 8, 9 and 10. However, other kinetics model failed to give straight lines in function vs. time plots.

Through liner regression of plots of $1-3(1-a)^{2/3}+2(1-a)$ vs. leaching duration of metals for different temperatures, rate constants could be calculated as shown in Tables 4, 5 and 6.

Table 4. The apparent rate constants of nickel at different temperatures

Leaching Temperature /K	T^{-1} /K^{-1}	Apparent rate constant k/min^{-1}	ln$k$
323	3.096×10^{-3}	1.73×10^{-3}	-6.36
333	3.003×10^{-3}	2.41×10^{-3}	-6.03
343	2.915×10^{-3}	3.15×10^{-3}	-5.76
353	2.833×10^{-3}	4.01×10^{-3}	-5.52

Table 5. The apparent rate constants of cobalt at different temperatures

Leaching Temperature /K	T^{-1} /K^{-1}	Apparent rate constant k/min^{-1}	ln$k$
323	3.096×10^{-3}	4.57×10^{-4}	-7.69
333	3.003×10^{-3}	6.36×10^{-4}	-7.36
343	2.915×10^{-3}	8.01×10^{-4}	-7.13
353	2.833×10^{-3}	1.19×10^{-3}	-6.73

Table 6. The apparent rate constants of manganese at different temperatures

Leaching Temperature /K	T^{-1} /K^{-1}	Apparent rate constant k/min^{-1}	ln$k$
323	3.096×10^{-3}	2.71×10^{-3}	-5.91
333	3.003×10^{-3}	4.17×10^{-3}	-5.48
343	2.915×10^{-3}	5.04×10^{-3}	-5.29
353	2.833×10^{-3}	6.81×10^{-3}	-4.99

The rate constant is a function of temperature. The relationship of rate constant k and temperature T could be expressed with Arrhenius equation:

$$\ln k = \ln A - \frac{E_a}{RT} \tag{4}$$

where A is the frequency factor and E_a is the apparent activation energy. The Arrhenius plots, which describe the relationship of rate constant and temperature, are shown in Figs. 11, 12 and 13. It can be found that the plots in these figures of ln$k$ against $1/T$ giving a straight line, which proves that the model applied is suitable. And the values of the activation energy calculated from the slope of these lines are 11.56 kJ/mol for nickel, 11.26 kJ/mol for cobalt and 10.77 kJ/mol for manganese, respectively. As verified in previous work, the optimum speed value is 300 rpm, and valuable metals extraction enhanced with the increase of the agitation speed from 100 to 300 rpm. However, less enhacement was obtained in higher speed (more than 300 rpm). It suggests that that the external diffusion effect is negligible at 300 rpm or above. Therefore, 300 rpm was chosen for the all experiments to ensure that the measured leaching rate was free from diffusion through the liquid film. In view of the negligible external diffusion effect at 300 rpm, we can speculate that the diffusion through the product layer is the

controlling step in the dissolution process of Ni, Co and Mn. Namely, the controlling step is diffusion through solid film.
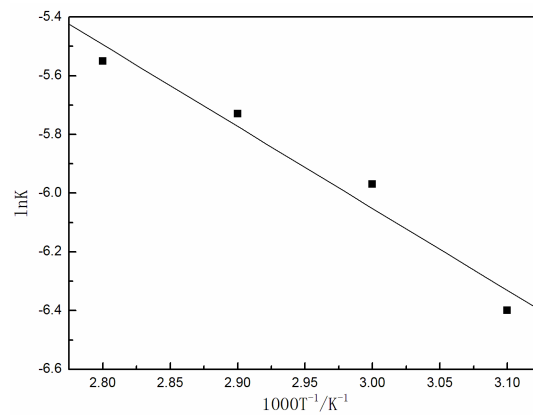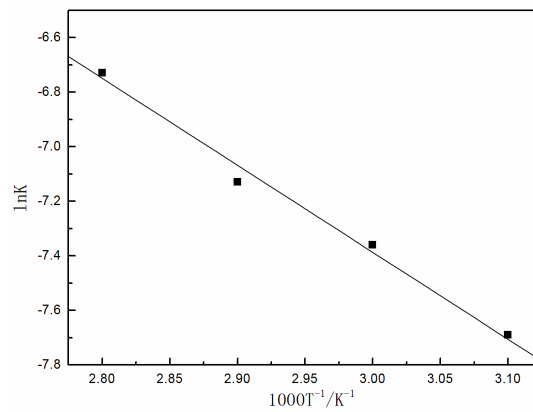

Fig. 11. The plot of ln$k$-T^{-1} of nickel
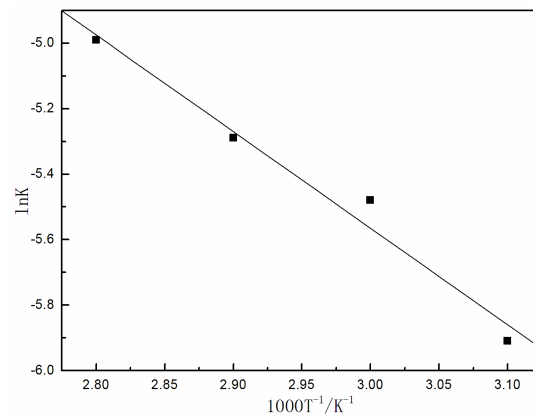

Fig. 12. The plot of ln$k$-T^{-1} of cobalt

Fig. 13. The plot of ln$k$-T^{-1} of manganese

3.3. Leaching Mechanism

As we all know, studing the mechanism benefits the kinetics analysis of valuable metals leaching. Through mineralogical analysis of the ore, it can be found that nickel and cobalt are distributed in different minerals and mainly in iron mineral and silicate mineral.

The leaching residues XRD diagram of different leaching time are shown in Fig. 14. Lizardite characteristic peaks at 2θ angle of 12.1°, 24.2° and 60.1° as shown in Fig. 14 are observed to become

weaker with the increase of leaching time. Composition analysis of the ore reveals that there is plenty of silicate in the ore, but only one characteristic peak at 2θ angle of 26.8° as shown in Figs. 2 and 14, which demonstrates that silicate is the amorphous phase or existed in weak crystal phase. What's more, it can be found there are bread peak from 14° to 30° in the XRD diagram of raw ore in Figs. 2 and 14. With the decomposition of lizardite, more and more silica releases, existing in new characteristic peak at 2θ angle of 20.1°. At the same time, the peak of 26.8° become sharper than before. And goethite mineral characteristic peaks at 2θ angle of 21°, 33.2°, 36.8° and 54.1° nearly disappear, when leaching duration is 0.5 h. It proves that goethite dissolves faster than lizardite under these leaching conditions.

Hematite is detectable in the residue by XRD at 2θ angle of 33.6° and 54.1°, which indicates that some hematite peaks can be observed only after the partially dissolution of goethite. The peaks of magnetite and hematite become weak but still exist in Fig. 14, even increasing the leaching duration upto 2 h. The absence of the goethite peak implies that goethite dissolves in preference to magnetite and hematite. Therefore, the order of the effect of these minerals dissolution is: goethite>lizardite>magnetite≈ hematite.

Due to the existence of silica, magnetite, hematite and talc, and some of them generated in the leaching process can form solid film, which hinder the leaching of valuable metals. Therefore, the rate-controlling step is inner diffusion in the leaching process of laterites, namely solid film diffusion controlling.
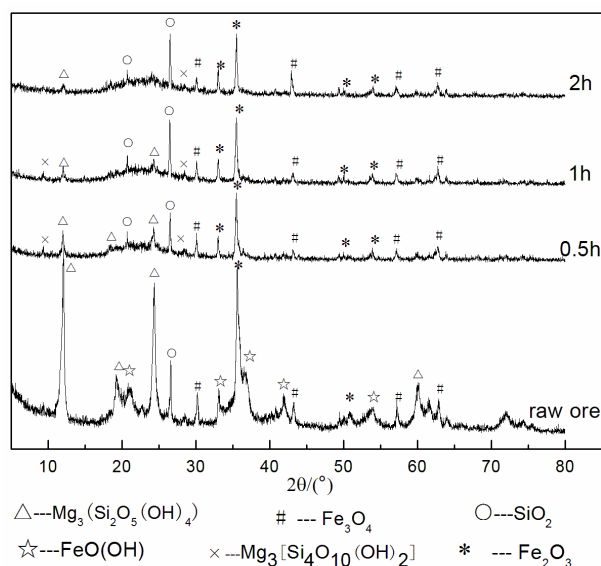

Fig. 14. The XRD diagram of leaching residues of different leaching time

4.   Conclusions

The ore employed in this paper was mixture from three layers of a mine, and the main valuable metals of nickel and cobalt are distributed in different minerals, such as goethite, limonite, sulfite and lizardite. The content of nickel and cobalt are not high in the above-mentioned ore. Analysis of optical microscope shows that the ore must be ground to small particle size, so as to increase the dissolution of valuable metals. Kinetics analysis shows that equation of $1-3(1-a)^{2/3}+2(1-a)=k_2 t$ is suitable, and the values of activation energy calculated from the Arrhenius plots of k_2 are 11.56 kJ/mol for nickel, 11.26 kJ/mol for cobalt and 10.77 kJ/mol for manganese. Combined with the analysis of leaching conditions and leaching mechanism, the controlling step is solid film diffusion controlling.

References

BUYUKAKINCI, E., TOPKAYA Y.A., 2009. *Extraction of nickel from lateritic ores at atmospheric pressure with agitation leaching*. Hydrometallurgy 97 (1-2), 33-38.

OLANIPEKUN, E. O., 2000. *Kinetics of leaching late*rite. Int. J. Miner. Process. 60 (1), 9-14.

FAN, C.L., ZHAI, X.J., FU, Y., CHANG, Y.F., LI, B.C., ZHANG, T.A., 2011. *Kinetics of selective chlorination of pre-reduced limonitic nickel laterite using hydrogen chloride*. Miner. Eng. 24 (9), 1016-1021.

HALLBERG, K.B., GRAIL, B.M, DU PLESSIS, C.A, JOHNSON, D.B., 2011. *Reductive dissolution of ferric iron minerals: A new approach for bio-processing nickel laterites*. Miner. Eng. 24 (7), 620-624.

MACCARTHY, J., NOSRATI, A., SKINNER, W., ADDAI-MENSAH, J., 2016. *Atmospheric acid leaching mechanisms and kinetics and rheological studies of a low grade saprolitic nickel laterite ore*. Hydrometallurgy 160, 26-37.

LAKSHMANAN, V.I., SRIDHAR, R., CHEN, J., HALIM, M.A., 2016. *Development of mixed-chloride hydrometallurgical processes for the recovery of value metals from various resources*. Trans. Indian Inst. Met., 1, 39-50.

LI, J.H., LI, Y.Y., ZHENG, S., XIONG, D.L., CHEN, H., ZHANG, Y.F., 2015. *Research review of laterite nickel ore metallurgy*. Nonferrous Metals Science and Engineering 6(1), 35-40.

LIU, K., CHEN, Q.Y., YIN, Z.L., HU, H.P., DING, Z.Y., 2012. *Kinetics of leaching of a Chinese laterite containing maghemite and magnetite in sulfuric acid solutions*. Hydrometallurgy 125-126, 125-136.

LIU, W.R., LI, X.H., HU, Q.Y., WANG, Z.X., GU, K.Z., LI, J.H., ZHANG, L.X., 2010. *Pretreatment study on chloridizing segregation and magnetic separation of low-grade nickel laterites*. Nonferrous Met. Soc. China 20, s82-s86.

MA, B.Z., YANG, W.J., YANG, B., WANG, C.Y., CHEN, Y.Q., ZHANG, Y.L., 2015. *Pilot-scale plant study on the innovative nitric acid pressure leaching technology for laterite ores*. Hydrometallurgy 155, 88-94.

MCDONALD, R.G., WHITTINGTON, B.I., 2008a. *Atmospheric acid leaching of nickel laterites review Part I. Sulphuric acid technologies*. Hydrometallurgy 91 (1–4), 35–55.

MCDONALD, R.G., WHITTINGTON, B.I., 2008b. *Atmospheric acid leaching of nickel laterites review. Part II. Chloride and bio-technologies*. Hydrometallurgy 91 (1–4), 56–69.

MUDD, G.M., 2010. *Global trends and environmental issues in nickel mining: Sulfides versus laterites*. Ore Geology Reviews, 38 (1-2), 9-26.

NORGATE, T., JAHANSHAHI, S., 2011. *Assessing the energy and greenhouse gas footprints of nickel laterite processing*. Miner. Eng., 24 (7), 698-707.

RICE, N.M., 2016. *A hydrochloric acid process for nickeliferous laterites*. Miner. Eng. 88, 28-52.

WEI, L., FENG, O., OU, L., ZHANG, G., CHEN, Y., 2010. *Kinetics of saprolitic laterite leaching by sulphuric acid at atmospheric pressure*. Miner. Eng. 23 (6), 458-462.

ZHANG, P.Y., GUO, Q., WEI, G.Y., MENG, L., HAN, L.X., QU, J.K., QI, T., 2016. *Leaching metals from saprolitic laterite ore using a ferric chloride solution*. J. Clean. Prod. 112, 3531-3539.

ZHANG, Q., WEN, S.M., FENG, Q.C., NIE, W.L., WU, D.D., 2017. *Dissolution kinetics of hemimorphite in methane sulfonic acid*. Physicochem. Probl. Miner. Process., doi: 10.5277/ppmp18105.

ZHAO, C.M., CAI, Y.H., NING, Z., WANG, G.C., KANG, S.M., ZHANG, C.M., ZHAI, Y.C., 2017. *Recovery of MgO from laterite nickel slag through roasting by ammonium sulfate*. Journal of Central South University (Science and Technology), 48 (8), 1972-1978.